Energy Landscape of Streptavidin−Biotin Complexes Measured by Atomic Force Microscopy†

Chunbo Yuan, Aileen Chen, Pamela Kolb, and Vincent T. Moy*

Department of Physiology and Biophysics, University of Miami School of Medicine, 1600 NW 10th Avenue, Miami, Florida 33136

Received November 29, 1999; Revised Manuscript Received June 16, 2000

ABSTRACT: The dissociation of ligand and receptor involves multiple transitions between intermediate states formed during the unbinding process. In this paper, we explored the energy landscape of the streptavidin−biotin interaction by using the atomic force microscope (AFM) to measure the unbinding dynamics of individual ligand−receptor complexes. The rupture force of the streptavidin−biotin bond increased more than 2-fold over a range of loading rates between 100 and 5000 pN/s. Moreover, the force measurements showed two regimes of loading in the streptavidin−biotin force spectrum, revealing the presence of two activation barriers in the unbinding process. Parallel experiments carried out with a streptavidin mutant (W120F) were used to investigate the molecular determinants of the activation barriers. From these experiments, we attributed the outer activation barrier in the energy landscape to the molecular interaction of the '3-4' loop of streptavidin that closes behind biotin.

To fully understand the role of ligand−receptor interactions in cell adhesion and de-adhesion, it is necessary to examine the dynamic response of individual ligand−receptor complexes to external mechanical forces. On the basis of the Bell model, one would expect that the application of mechanical pulling force would reduce the activation energy barrier of a ligand−receptor complex toward dissociation and, hence, would reduce the lifetime of the complex (*1*, *2*). Moreover, an increase in the rate of force application should increase the rupture force of the ligand−receptor bond. To test and refine the proposed models, studies based on direct force measurements are essential.

Direct measurements of ligand−receptor interactions can be obtained using different biophysical approaches, including the use of the optical tweezers, the magnetic torsion device, the biomembrane force probe (BFP),[1] and the atomic force microscope (AFM) (*3*−*6*). Specifically, the AFM and the BFP have been employed to characterize the unbinding force of individual ligand−receptor complexes (*7*−*14*). Moreover, recent studies have shown that direct force measurements can be used to explore the energy landscape of ligand−receptor unbinding (*9*).

The streptavidin−biotin system is particularly well-suited for direct force measurement studies of ligand−receptor bonds (*7*, *9*, *15*−*18*). The wide interest in this model system stems from its high affinity and specificity of interaction (*19*) and the availability of structural (*20*, *21*) and biophysical data (*22*). Streptavidin is a tetrameric protein with each of the four identical subunits capable of binding one biotin molecule. The crystal structure of the streptavidin−biotin complex revealed that each subunit is formed by a single polypeptide chain arranged in an eight-stranded antiparallel β-barrel structure to which biotin binds. The streptavidin−biotin complex is stabilized by an elaborate network of hydrogen bonds and van der Waals interactions, including a contribution from tryptophan 120 of an adjacent streptavidin monomer (*20*, *21*, *23*).

Recently, Merkel et al. reported that the strength of an individual streptavidin−biotin complex increased gradually with the logarithm of the loading rate (*9*). These measurements also revealed that the streptavidin−biotin complex undergoes multiple transitions before final separation. The current study was undertaken to explore the molecular determinants of the transition states.

MATERIALS AND METHODS

Functionalization of AFM Tips. Si_3N_4 cantilevers were functionalized with streptavidin (or its analogues or avidin) as follows (*24*): Si_3N_4 tips were immersed in acetone for 5 min and then irradiated with ultraviolet light for 30 min. The irradiated tips were incubated in 50 μL of biotinylated bovine serum albumin (biotin-BSA; Pierce, Rockford, IL; 0.5 mg/mL in 100 mM $NaHCO_3$, pH 9) overnight at 37 °C and then rinsed six times with phosphate buffered saline (PBS; 20 mM PO_4^{3-}, 150 mM NaCl, pH 7.2). Streptavidin was coupled to the tips during a 5-min incubation in 50 μL of streptavidin (0.5 mg/mL in PBS) at room temperature. The streptavidin functionalized tips were used immediately in measurements after rinsing with PBS to remove unbound streptavidin molecules. Avidin (NeutrAvidin), streptavidin, and biotin-BSA were purchased from Pierce. W120F was purified according to Sano and Cantor (*25*).

† This work was supported by the American Cancer Society and the NIH (1 R29 GM55611-01).

* To whom correspondence should be addressed. Phone: (305) 243-3201. Fax: (305) 243-5931. E-mail: vmoy@newssun.med.miami.edu.

[1] Abbreviations: atomic force microscope, AFM; biomembrane force probe, BFP; phosphate buffered saline, PBS; bovine serum albumin, BSA.

10.1021/bi992715o CCC: $19.00
Published on Web 07/27/2000

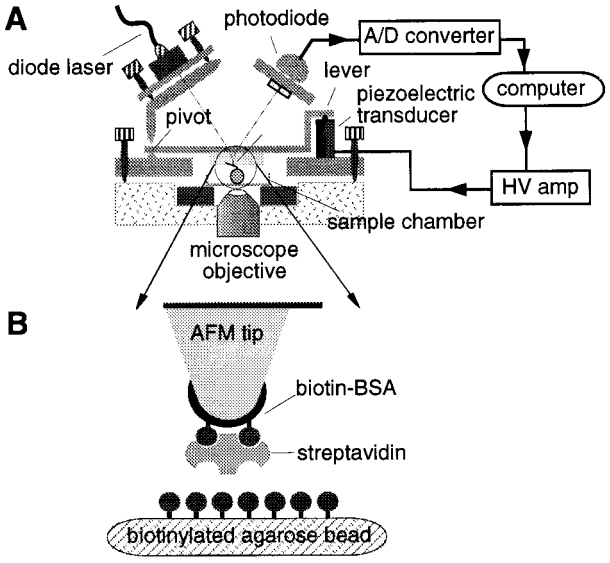

FIGURE 1: (A) Schematic representation of the atomic force apparatus used to measure the dynamic strength of the streptavidin−biotin bonds. (B) Schematic representation of a streptavidin-functionalized AFM tip and the surface of a biotinylated agarose bead.

AFM Force Measurements. All force measurements were performed using an atomic force apparatus (Figure 1); its design and operation are similar to the conventional AFM. A piezo translator with a strain gauge position sensor (Physik Instrumente, Waldbronn, Germany) was used to rotate a lever which in turn set the position of the AFM tip relative to the substrate. The interaction between the AFM tip and the substrate was determined from deflection of the AFM cantilever. To monitor the cantilever's deflection, a focused laser spot from a pig-tailed diode laser (Oz Optics, Ontario, Canada) was reflected off the reverse side of the cantilever onto a two-segment photodiode. The photodiode signal was preamplified, digitized by a 16-bit analog-to-digital converter (Instrutech Corp., Port Washington, NY), and processed by an Apple computer that also controlled and recorded the events of the measurements. The force apparatus was equipped with an inverted optical system to assist in localizing the biotinylated agarose beads (Sigma, St. Louis, MO) and positioning of the functionalized AFM tip over the center of agarose beads. To minimize mechanical noise and temperature fluctuations, the force apparatus was suspended inside of a large emptied refrigerator.

To vary the loading rate in the force measurements, three sizes of silicon nitride cantilevers were used [cantilevers A, C, and D from unsharpened, gold-coated Microlever (MLCT-AUHW), ThermoMicroscopes, Sunnyvale, CA]. Each cantilever was individually calibrated by thermal fluctuation analysis to determine its spring constant (*26*). The measured spring constants of the cantilevers did not vary significantly from the nominal values given by the manufacturer and were in the range of 10 to 50 mN/m. The deflection of the cantilever was calibrated using the Petri dish surface as reference. The scan speed of the force measurement was determined from the rate of piezo expansion and was in the range of 40−1000 nm/s. All AFM force measurements were carried out in PBS. The temperature of the experimental system was continuously monitored and maintained at 25 ± 1 °C.

Expression and Purification of W120F. W120F is a truncated form of streptavidin (aa. 16−133) with a substitution at residue 120 (Trp to Phe). Expression and purification of W120F were described elsewhere (*25*). Briefly, oligonucleotide-directed mutagenesis was performed on wild-type streptavidin gene using a 30-base oligonucleotide to convert the codon for Trp-20 (TGG) to TCC for Phe. An expression vector containing the W120F gene, the bacteriophage T7 gene Φ10 promoter, and the bacteriophage T7 transcription terminator was used to transform *Escherichia coli*.

W120F was purified from overnight cultures inoculated with the transformed bacteria. Four hours after induction with isopropylthio-β-D-galactoside (1mM), the cells were pelleted and then resuspended in a lysis buffer containing a cocktail of protease inhibitors. The cell lysate was treated with DNAase I and RNAase I for 30 min and centrifuged to isolate the inclusion body fraction. The precipitate was dissolved in 6 M guanidine hydrochloride (pH 1.5)/10 mM DTT to solublize the expressed protein. To promote the refolding of the denatured proteins, the fraction was dialyzed against four changes of 0.2 M ammonium acetate (pH 6.0) plus protease inhibitors. The pH of the dialyzed sample was adjusted to 10.5 before it was applied to a 2-iminobiotin agarose column. Bound W120F was eluted with 6 M urea and 50 mM ammonium acetate (pH 4.0). The purified W120F was neutralized and stored at −70 °C.

RESULTS

Force measurements of the streptavidin−biotin interactions were carried out using an AFM in the force scan mode (Figure 1A) (*7*, *15*). For these experiments, an AFM tip, coated with streptavidin (Figure 1B), was brought in contact with an agarose bead coupled with biotin. The adhesive force of streptavidin−biotin interaction was measured as the AFM tip retracted from the surface of the bead. The specificity of this interaction was demonstrated with addition of free streptavidin or biotin, both of which abolished adhesion. It is unlikely that the breakage had occurred elsewhere in this system besides the streptavidin−biotin bond, since we were able to obtain hundreds and frequently thousands of measurements before the activity of the streptavidin tip was completely lost. If the BSA−tip interaction were to unbind during the measurements, we would not have been able to acquire as many measurements as we did. The total number of streptavidin−biotin bonds formed in a given measurement depended on receptor density, the duration of contact, and the area of contact. As in shown Figure 2A, the retract trace of the force measurement may exhibit several transitions in force due to the sequential unbinding of multiple streptavidin−biotin complexes. The rupture force of these linkages was determined from the magnitude of the measured transitions and usually corresponded to the applied force needed to break one or two bonds.

The rupture force of the streptavidin−biotin complex was measured at different force loading rates. Variation in the loading rate $\dot{f}$ of the AFM measurements was achieved with different combinations of AFM cantilevers and cantilever retraction rates, v_c. $\dot{f}$ is the product of the system spring constant, k_s and v_c, i.e., $\dot{f} = k_s \times v_c$. The system spring constant depends on the elastic properties of both the cantilever and the agarose filament to which biotin is

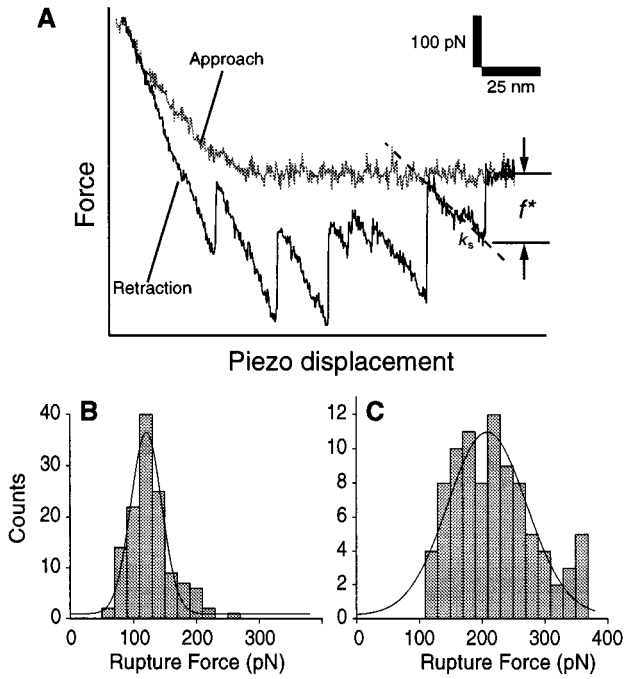

FIGURE 2: (A) Force vs displacement curves of the interaction between a streptavidin-functionalized tip and a biotinylated agarose bead. The measurement recorded the force on the AFM cantilever on approach and retraction of the cantilever from the agarose bead. f^* is the rupture force. k_S is the slope of the force vs displacement curve. The measurement was carried out with a cantilever spring constant of 30 mN/m and a scan speed, ν_c, of 600 nm/s. Each cantilever was individually calibrated by thermal fluctuation analysis to determine its spring constant (*26*). Histograms of the adhesion force between a streptavidin tip and biotin bead at loading rates of (B) 198 pN/s (k_S = 2.3 mN/m and ν_c = 86 nm/s) and (C) 2300 pN/s (k_S = 2.3 mN/m and ν_c = 1 μm/s). Both histograms were fitted to a Gaussian function (*2*). The centers of the force distribution (B) and (C) are 126 ± 2.3 (SEM) pN (N = 256) and 207 ± 5.8 (SEM) pN (N = 100), respectively. All AFM force measurements were carried out in PBS and at 25 ± 1 °C.

attached. The measured system spring constants were in the range of 1.5−3.0 mN/m and were obtained from the slope of the force vs displacement relationship of the retract trace (Figure 2A). Three different types of cantilevers were used. Although the spring constants (10, 30, and 50 mN/m) of the cantilevers varied by a factor of 5, only a 2-fold change in the system spring constant was observed since the elasticity of the agarose filament is much smaller than the spring constant of the cantilever and, hence, dictated the system spring constant. Consequently, the loading rate of the force measurements was determined primarily by the rate of cantilever retraction, which was varied from 40 to 1000 nm/s.

The mean rupture force of the streptavidin−biotin complex at a given loading rate was determined from a force histogram of >100 measurements. To ensure that adhesion was mediated by a single streptavidin−biotin bond, the force exerted on the cantilever approach was regulated so that approximately 25% of the trials resulted in adhesion. Under these conditions, the probability that adhesion was mediated by a single streptavidin−biotin bond was >85% (*9*). Figure 2, panels B and C show force histograms obtained at loading rates of 198 and 2300 pN/s, respectively. The corresponding mean rupture forces, obtained by fitting the histogram to a Gaussian function, were 126 ± 2.3 (SEM) pN (N = 256) and 207 ± 5.8 (SEM) pN (N = 100), respectively. Figure 3

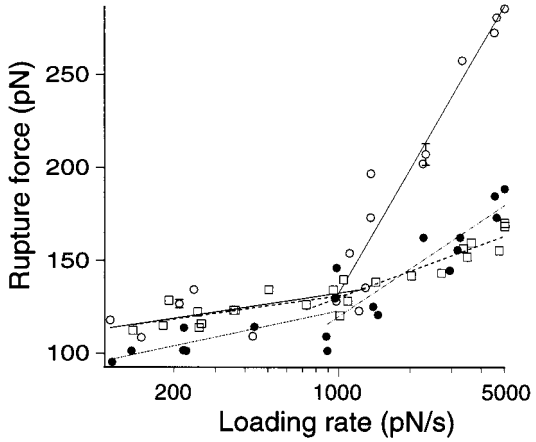

FIGURE 3: Loading rate dependence of the rupture force in the unbinding of the streptavidin−biotin (○), avidin−biotin (□), and W120F−biotin (●). Both regimes in force spectra were fitted to the Bell model. Standard errors of all data points were less than 5% of the mean value. Representative error bars were placed on selected data points.

plots the mean rupture force against the loading rate for the interaction of biotin with streptavidin and its analogues. W120F is a variant of streptavidin generated by site-specific mutagenesis of trytophan 120 to phenylalanine (*23*). Avidin is a homologue of streptavidin with structural and biotin binding properties similar to streptavidin (*27*). The rupture force of the streptavidin−biotin complex was most sensitive to changes in loading rate, displaying a greater than 2-fold increase in rupture force over the range of loading rates examined.

DISCUSSION

Figure 3 summarizes the dynamic response of three streptavidin (analogue)−biotin pairs to loading rates between 100 and 5000 pN/s. Within this range of loading rates, the rupture force of the complexes showed an initial gradual increase, followed by a more rapid increase with increasing loading rates. At the slower loading, the dynamic response of the streptavidin−biotin and avidin−biotin complexes overlapped. However, at faster loading rates >1000 pN/s, the streptavidin−biotin complex was able to support a larger load than the avidin−biotin complex, an observation consistent with previously reported results (*15*−*17*). This difference in the rupture force of the streptavidin−biotin and avidin−biotin bonds has been attributed to the differences in the activation enthalpy of the two complexes (*15*, *17*).

The force measurements summarized in Figure 3 can also be examined in the context of the Bell model (*1*, *2*). According to Bell, the dissociation rate k of a bond is amplified by the application of an external force f as follows:

$$k(f) = k^\circ \exp[fx_\beta/k_BT] \quad (1)$$

Here, k° is the dissociation rate constant in the absence of applied force, k_B is Boltzmann's constant, and x_β is a parameter that characterizes the relationship between force and dissociation rate. Assuming that the bond dissociation is a random process, the probability density function for failure of a single linkage at time t is given by (*28*)

$$p(t,f) = k(f) \exp\left\{-\int_0^t k(f(t'))dt'\right\} \quad (2)$$

Table 1: Bell Model Parameters from f^* vs log (r_f) Relation

ligand−receptor pair	loading rate range (pN/s)	x_β (nm)	k° (s^{-1})	$\Delta\Delta E^a$ (k_BT)
streptavidin−biotin	100−1000	0.49	1.67×10^{-5}	
	1000−5000	0.05	2.09	
avidin−biotin	100−1000	0.53	6.45×10^{-6}	0.95
	1000−5000	0.20	0.08	3.26
W120F−biotin	100−1000	0.31	6.70×10^{-3}	−5.99
	1000−5000	0.11	1.05	0.69

[a] $\Delta\Delta E$ is relative to streptavidin-biotin binding energy.

By setting dp/df, one can determine the maximum of the density function. The corresponding force f^* for a linear increase in force (i.e., $f = r_f t$; $r_f \equiv$ force loading rate) is given by

$$k(f^*) = r_f \frac{\partial}{\partial f} \ln k(f)\Big|_{f=f^*} \quad (3)$$

Substituting eq 1 into eq 3 gives

$$f^* = \frac{k_B T}{x_\beta} \ln\left(\frac{x_\beta}{k^\circ k_B T}\right) + \frac{k_B T}{x_\beta} \ln(r_f) \quad (4)$$

The Bell model thus predicts a linear relationship between the rupture force and logarithm of the loading rate.

As shown in Figure 3, the force spectrum of the streptavidin−biotin bond revealed two regimes within the range of the experimental loading rates. This observed change in the slope of f^* vs log(r_f) can be attributed to the suppression of an outer energy barrier of the energy landscape (*2*). Thus, in contrast to the simple Bell model, the data revealed that the streptavidin−biotin complex overcomes two transitions, an inner barrier and an outer barrier, during its unbinding.

The force measurements can be used to obtain an estimate of the relative change in the outer and inner activation energy barriers between the streptavidin−biotin pair and its analogues. The Bell model parameters of both transitions were determined for the different ligand−receptor pairs by fitting the force measurements to eq 4 and are tabulated in Table 1. According to transition state theory, the dissociation rate is a function of the activation energy ΔE (i.e., $k \propto \exp[-\Delta E/kT]$). The difference in activation energy between two homologous systems [i.e., $\Delta\Delta E = \Delta E$(mut) − ΔE(w.t.), where ΔE(w.t.) is the transition energy of wild-type streptavidin and ΔE(mut)] is the corresponding transition energy of a streptavidin mutant can be obtained from the ratio of the dissociation rates (i.e., $k_{mut}/k_{wt} = \exp\{-\Delta\Delta E/kT\}$). Table 1 tabulates the difference energies of the inner and outer barriers of the avidin−biotin and W120F−biotin pairs relative to the streptavidin−biotin pair. Our analysis revealed that the enhanced stability of the avidin−biotin complex may be attributed to a larger inner activation energy barrier of ∼3 kT (*27*, *29*). In contrast, the W120F−biotin complex is destabilized by the lowering of the outer activation energy barrier ($\Delta\Delta E \sim$ 6kT) as illustrated in Figure 4.

On the basis of the analysis of molecular dynamic (MD) simulations (*30*, *31*) and direct force measurements, Merkel et al. (*9*) proposed that the outer barrier in the energy landscape of the streptavidin−biotin emanates from the interaction of the '3-4' loop, which closes behind the bound biotin. To test this hypothesis, we compared the force spectra

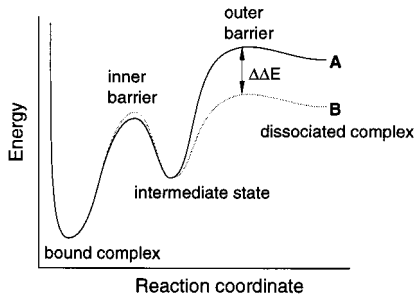

FIGURE 4: Conceptual energy landscapes of the (A) streptavidin−biotin interaction and the (B) W120F−biotin interaction.

obtained from the streptavidin−biotin and W120F−biotin interactions. The W120F mutant differed from wild-type streptavidin by a point mutation at the '3-4' loop. A consequence of this substitution is a reduction in binding (free) energy of ∼4.6 kT (*22*). As summarized in Table 1, the AFM force measurements attributed the difference in binding energies to a reduction in the transition energy of the outer barrier ($\Delta\Delta E = 6$ kT) and, as predicted, there was minimal change in the energy of the inner barrier ($\Delta\Delta E =$ 0.69 kT).

In summary, our results demonstrate that the strength of biological linkages can vary by a considerable amount, depending on the rate of force application. Moreover, we introduced a general approach for identifying the molecular determinants of an energy landscape by comparing force measurements of native receptor with mutated receptors. Together with MD simulations, this approach can greatly enhance our understanding of bimolecular unbinding.

ACKNOWLEDGMENT

We thank Y. Jiao, H. Wu, M. Schmidt, T. Kuhn, S. Sutter, and C. Freites for technical support and T. Sano for the W120F-expressing cells.

REFERENCES

1. Bell, G. I. (1978) *Science 200*, 618−627.
2. Evans, E., and Ritchie, K. (1997) *Biophys. J. 72*, 1541−1555.
3. Stout, A. L., and Webb, W. W. (1998) *Methods Cell Biol. 55*, 99−116.
4. Wang, N., Butler, J. P., and Ingber, D. E. (1993) *Science 260*, 1124−1127.
5. Evans, E., Ritchie, K., and Merkel, R. (1995) *Biophys. J. 68*, 2580−2587.
6. Binnig, G., Quate, C. F., and Gerber, C. (1986) *Phys. Rev. Lett. 56*, 930−933.
7. Florin, E. L., Moy, V. T., and Gaub, H. E. (1994) *Science 264*, 415−417.
8. Lee, G. U., Chrisey, L. A., and Colton, R. J. (1994) *Science 266*, 771−773.
9. Merkel, R., Nassoy, P., Leung, A., Ritchie, K., and Evans, E. (1999) *Nature 397*, 50−53.
10. Allen, S., Davies, J., Davies, M. C., Dawkes, A. C., Roberts, C. J., Tendler, S. J., and Williams, P. M. (1999) *Biochem. J. 341*, 173−178.
11. Fritz, J., Katopodis, A. G., Kolbinger, F., and Anselmetti, D. (1998) *Proc. Natl. Acad. Sci. U.S.A. 95*, 12283−12288.
12. Hinterdorfer, P., Baumgartner, W., Gruber, H. J., Schilcher, K., and Schindler, H. (1996) *Proc. Natl. Acad. Sci. U.S.A. 93*, 3477−3481.
13. Dammer, U., Popescu, O., Wagner, P., Anselmetti, D., Guntherodt, H. J., and Misevic, G. N. (1995) *Science 267*, 1173−1175.
14. Shao, J. Y., and Hochmuth, R. M. (1999) *Biophys. J. 77*, 587−596.

15. Moy, V. T., Florin, E. L., and Gaub, H. E. (1994) *Science 266*, 257−259.
16. Lee, G. U., Kidwell, D. A., and Colton, R. J. (1994) *Langmuir 10*, 354−361.
17. Chilkoti, A., Boland, T., Ratner, B. D., and Stayton, P. S. (1995) *Biophys. J. 69*, 2125−2130.
18. Wong, S. S., Joselevich, E., Woolley, A. T., Cheung, C. L., and Lieber, C. M. (1998) *Nature 394*, 52−55.
19. Green, N. M. (1990) *Methods Enzymol. 184*, 51−67.
20. Weber, P. C., Ohlendorf, D. H., Wendoloski, J. J., and Salemme, F. R. (1989) *Science 243*, 85−88.
21. Hendrickson, W. A., Pähler, A., Smith, J. L., Satow, Y., Merritt, E. A., and Phizackerley, R. P. (1989) *Proc. Natl. Acad. Sci. U.S.A. 86*, 2190−2194.
22. Chilkoti, A., and Stayton, P. S. (1995) *J. Am. Chem. Soc. 117*, 10622−10628.
23. Sano, T., and Cantor, C. R. (1995) *Proc. Natl. Acad. Sci. U.S.A. 92*, 3180−3184.
24. Moy, V. T., Florin, E.-L., and Gaub, H. E. (1994) *Colloids Surf. 93*, 343−348.
25. Sano, T., and Cantor, C. R. (1990) *Proc. Natl. Acad. U.S.A. 87*, 142−146.
26. Hutter, J. L., and Bechhoefer, J. (1994) *Rev. Sci. Instrum. 64*, 1868−1873.
27. Green, N. M. (1975) *Adv. Protein Chem. 29*, 85−133.
28. Evans, E., Berk, D., and Leung, A. (1991) *Biophys. J. 59*, 838−848.
29. Weber, P. C., Wendoloski, J. J., Pantoliano, M. W., and Salemme, F. R. (1992) *J. Am. Chem. Soc. 114*, 3197−3200.
30. Grubmüller, H., Heymann, B., and Tavan, P. (1996) *Science 271*, 997−999.
31. Izrailev, S., Stepaniants, S., Balsera, M., Oono, Y., and Schulten, K. (1997) *Biophys. J. 72*, 1568−1581.

BI992715O